

E. Magyari · P. D. Weidman

The preheated Airy wall jet

Received: 25 June 2004 / Accepted: 13 January 2005 / Published online: 16 June 2005
 © Springer-Verlag 2005

Abstract The Airy jet is a wall-bounded flow belonging to the similarity class of the well known free jet but, in contrast to the latter, its far field behavior is an algebraically decaying rotational flow. The velocity and temperature distributions of a preheated Airy jet flowing over an insulated wall are investigated using both analytical and numerical methods, and are compared with those of the classical (preheated) exponentially decaying wall jet. For the same value of the dimensionless skin friction parameter, the maximum of the similar velocity profile of the Airy jet exceeds that of the classical wall jet by approximately 20%. The dimensionless temperature along the insulated wall scales for large values of the Prandtl number with $Pr^{2/3}$ for both jets, while for small values of the Prandtl number the temperature scales with $Pr^{1/3}$ for the Airy jet and goes to 1 for the classical wall jet.

List of symbols

Ai, Bi	Airy functions
c_p	Specific heat at constant pressure
$f(\eta)$	Similarity streamfunction variable
$g(\eta)$	Similarity temperature variable
G	Normalized temperature variable
J	Integral invariant for the classical wall jet
L	Length scale

M	Streamwise momentum flux
m, n	Streamwise power law exponents
Pr	Prandtl number
Q	Convected heat flux
S	Dimensionless skin friction
T	Temperature
T^*	Reference temperature
u, v	Velocity components
x, y	Cartesian coordinates
z	Argument of the Airy functions

Greek symbols

α	Power law exponent
β	Scale factor
γ	Scale factor; also Euler's constant
Γ	Gamma function
η	Independent similarity variable
θ	Modified similarity temperature variable
κ	Thermal diffusivity
μ	Dynamic viscosity
ν	Kinematic viscosity
ρ	Density
ψ	Streamfunction; also Digamma function

Subscripts

max	Maximum value
w	Wall condition
0	Jet slot condition
∞	Far field condition

Superscripts

'	Derivative with respect to η or z
---	--

This work is dedicated to Michael B. Glauert who passed away on June 14, 2004

E. Magyari (✉)
 Chair of Physics of Buildings, Institute of Building Technology,
 Swiss Federal Institute of Technology (ETH) Zürich, 8093 Zurich,
 Switzerland
 E-mail: magyari@hbt.arch.ethz.ch
 Tel.: +41-1-6332867
 Fax: +41-1-6331041

P. D. Weidman
 Department of Mechanical Engineering, University of Colorado,
 Boulder, CO 80309-0427, USA

1 Introduction

The zero pressure gradient shear driven flows, like the wall-driven Couette-flow, the wind-driven Ekman-flow,

the Lock-type flow near to the interface of two parallel streams etc. belong to the classical topics of fluid mechanics. Due to their wide technical and environmental applications, general research in shear driven flows is still of current interest. Recently, the adjustment of a zero pressure gradient laminar flow near a flat impermeable boundary to an exterior rotational flow of power-law velocity profile $U_\infty(y) = \beta y^{-\alpha}$ ($y \rightarrow \infty$, $\beta > 0$), where y is the flow transverse coordinate, has been investigated by Weidman et al. [1] for a wide range of values of α . An outstanding member of this family of wall bounded flows is the Airy wall jet corresponding to the value $\alpha = 1/2$ of the power-law exponent. The mechanical characteristics of this algebraically decaying wall jet have been considered by Weidman et al. [1] for impermeable flat plates and subsequently by Magyari et al. [2] and Magyari and Keller [3] for permeable surfaces. Their thermal characteristics for the non-preheated case were reported by Magyari et al. [4]. The goal of the present investigation is to compare the flow and thermal characteristics of a preheated Airy wall jet with the preheated classical wall jet, both streaming over a thermally insulated flat plate. The classical wall jet, commonly known as the Glauert jet, was actually first studied by Tetervin [5] in 1948, and then rediscovered independently by Akatnov [6] in 1953 and again by Glauert [7] in 1956. For this reason, especially to call attention to the less well known work of Tetervin [5], the classical wall jet will be referred to hereforth as the Tetervin-Akatnov-Glauert wall jet, or TAG jet for short. The thermal characteristics of the preheated radial jet have been studied by Riley [8], as part of a broader study on compressible wall jets with viscous dissipation, and also by Schwarz and Caswell [9] for the planar case.

2 Governing equations

We formulate the general problem for thermally active wall jets using streamwise and wall-normal Cartesian coordinates (x, y) whose corresponding velocity components are (u, v) . A planar wall jet, of incoming heat flux Q per unit span, issues through a narrow slot at $x=0$ over an insulated plate into the host fluid of ambient temperature T_∞ . For incompressible flow in the boundary layer approximation, neglecting buoyancy and viscous self-heating effects, the dimensional equations governing conservation of mass, momentum and energy are

$$u_x + v_y = 0 \quad (1a)$$

$$uu_x + vu_y = \nu u_{yy} \quad (1b)$$

$$uT_x + vT_y = \kappa T_{yy}, \quad (1c)$$

where ν and κ are the momentum and thermal diffusivities, respectively, and subscripts denote partial derivatives with respect to a coordinate. The flow and

thermal boundary conditions of interest in this study are

$$u = 0, \quad v = 0, \quad T_y = 0 \quad (y = 0) \quad (2a, b, c)$$

$$u \rightarrow 0, \quad T \rightarrow T_\infty \quad (y \rightarrow \infty). \quad (2d, e)$$

In addition, the incoming flow through the slit at $x=0$ has uniform temperature greater than the ambient and therefore a positive advected heat flux. Since the wall is insulated, and there is no loss of heat to the host fluid at infinity, it is clear that the heat flux Q must be independent of x . Mathematically, this result is obtained by multiplying Eq. 1c by $\rho c_p u$, integrating across the flow, and making use of Eq. 1a and thermal boundary conditions (2c, e) to obtain

$$Q = \rho c_p \int_0^\infty u(T - T_\infty) dy \quad (3)$$

as the thermal integral invariant.

3 Similarity formulation

Since the flow is incompressible it is convenient to introduce a streamfunction $(u, v) = (\psi_y, -\psi_x)$ and write the governing equations and boundary conditions as

$$\psi_y \psi_{xy} - \psi_x \psi_{yy} = \nu \psi_{yyy} \quad (4a)$$

$$\psi_y = 0, \quad \psi_x = 0 \quad (y = 0); \quad \psi_y \rightarrow 0 \quad (y \rightarrow \infty) \quad (4b, c, d)$$

$$\psi_y T_x - \psi_x T_y = \kappa T_{yy} \quad (5a)$$

$$Q = Q_0 \quad (x = 0), \quad T_y = 0 \quad (y = 0), \quad T \rightarrow T_\infty \quad (y \rightarrow \infty). \quad (5b, c, d)$$

A unified similarity formulation for thermally active wall jets is presented to show how the TAG, Airy and a further algebraically decaying wall jet arise as special cases corresponding to two different types of self-similar solutions of the boundary value problem (Eqs. 4). This approach has the benefit of exposing, at each stage of the development, similarities and differences between these preheated jet flows. A suitable general similarity ansatz is given by

$$\psi(x, y) = \frac{2\nu}{m+1} \left(\frac{x}{L}\right)^{(m+1)/2} f(\eta) \quad (6a)$$

$$T = T_\infty + T^* \left(\frac{x}{L}\right)^n g(\eta) \quad (6b)$$

$$\eta = \left(\frac{x}{L}\right)^{(m-1)/2} \frac{y}{L}. \quad (6c)$$

where L is a reference length, T^* is a reference temperature and $m \neq -1$. The dimensional velocities are then

$$u = \frac{2}{(m+1)L} \frac{v}{L} \left(\frac{x}{L}\right)^m f'(\eta) \quad (7a)$$

$$v = -\frac{v}{L} \left(\frac{x}{L}\right)^{(m-1)/2} \left[f(\eta) + \frac{m-1}{m+1} \eta f'(\eta) \right]. \quad (7b)$$

Inserting Eq. 6 into Eqs. 4 and 5 furnishes the boundary-value problem for the flow variable

$$f''' + ff'' - \frac{2m}{m+1} f'^2 = 0 \quad (8a)$$

$$f(0) = 0, \quad f'(0) = 0; \quad f'(\eta) \rightarrow 0 \quad (\eta \rightarrow \infty) \quad (8b, c, d)$$

and the coupled boundary-value problem for the similar temperature variable

$$\frac{1}{Pr} g'' + fg' - \frac{2n}{m+1} f'g = 0 \quad (9a)$$

$$g'(0) = 0, \quad g(\eta) \rightarrow 0 \quad (\eta \rightarrow \infty) \quad (9b, c)$$

where a prime denotes differentiation with respect to η and $Pr = \nu/\kappa$ is the Prandtl number.

4 Flow solutions: algebraic and exponential jets

For immediate reference, it is worth observing that the flow equation 8a may be written in the form

$$\frac{d^2}{d\eta^2} \left(f' + \frac{1}{2} f^2 \right) - \frac{1+3m}{1+m} f'^2 = 0 \quad (10a)$$

or, alternatively, as

$$f^{-1} \frac{d}{d\eta} \left[f^{\frac{3}{2}} \frac{d}{d\eta} \left(f^{-\frac{1}{2}} f' + \frac{2}{3} f^{\frac{3}{2}} \right) \right] - \frac{2(1+2m)}{1+m} f'^2 = 0. \quad (10b)$$

These equations show that the values $m = -1/3$ and $m = -1/2$ of the exponent m which governs the streamwise scale of the self similar flows described by boundary layer equations (1a, b) play a special role unrelated to the boundary conditions. They are the so-called “nonlinear eigenvalues” [10] of Eq. 8a which are associated with particular conserved flow quantities. These conserved quantities, first integrals of second order, are

$$\frac{d}{d\eta} \left(f' + \frac{1}{2} f^2 \right) = C_1 \quad (11a)$$

and

$$f^{\frac{3}{2}} \frac{d}{d\eta} \left(f^{-\frac{1}{2}} f' + \frac{2}{3} f^{\frac{3}{2}} \right) = C_2 \quad (11b)$$

corresponding to $m = -1/3$ and $m = -1/2$, respectively.

The far field condition (Eq. 8d) implies that

$$C_1 = \lim_{\eta \rightarrow \infty} [f(\eta) f'(\eta)] \quad (12a)$$

and

$$C_2 = \lim_{\eta \rightarrow \infty} [f^2(\eta) f'(\eta)]. \quad (12b)$$

If the similar jet velocity $f'(\eta)$ decays exponentially as $\eta \rightarrow \infty$, we have $C_1 = C_2 = 0$ and thus a further integration of Eqs. 11a and b is possible. This yields the first order equations

$$f' + \frac{1}{2} f^2 = C_3 \quad (m = -1/3) \quad (13a)$$

$$f^{-\frac{1}{2}} f' + \frac{2}{3} f^{\frac{3}{2}} = C_4 \quad (m = -1/2). \quad (13b)$$

From Eq. 13a and far field condition (Eq. 8d) one obtains $C_3 = f_\infty^2$ where $f_\infty \equiv f(\infty)$ is the (dimensionless) entrainment velocity for this flow. Thus in Eq. 13a we recover the well known Schlichting-Bickley free jet solution [11, 12]

$$f(\eta) = f_\infty \tanh\left(\frac{f_\infty}{2} \eta\right) \quad (m = -1/3) \quad (14)$$

with the center plane property $f''(0) = 0$. As Bickley [12] pointed out, f_∞ can be determined uniquely by specifying the incoming momentum flux

$$M = \rho \int_0^\infty u^2 dy \quad (15)$$

in the free jet. In this way, Eqs. 7a, 14 and 15 yield

$$f_\infty = \left(\frac{3M}{16L\rho v^2} \right)^{1/3} \quad (m = -1/3). \quad (16)$$

Similarly, the far field condition (Eq. 8d) applied to Eq. 13b gives $C_4 = (2/3)f_\infty^{3/2}$, and hence

$$f' = \frac{2}{3} f_\infty^2 \left[\left(\frac{f}{f_\infty} \right)^{1/2} - \left(\frac{f}{f_\infty} \right)^2 \right] \quad (m = -1/2) \quad (17)$$

in which one recognizes the basic equation of the TAG wall jet [5–7]. Using wall conditions (Eq. 8b, c) and Eq. 17, the constant f_∞ in this case can be related to the dimensionless skin friction parameter $S \equiv f''(0)$ as follows

$$f_\infty = \left(\frac{9S}{2} \right)^{1/3} \quad (m = -1/2). \quad (18)$$

Furthermore, a relationship necessary to determine f_∞ and S uniquely can be obtained by specifying the “flux

of the exterior momentum flux” of the TAG jet, i.e. the conserved quantity [6, 7]

$$J = \rho^2 \int_0^\infty u \left(\int_y^\infty u^2 dy \right) dy. \quad (19)$$

In this way, Eqs. 7a, 17 and 19 yield

$$f_\infty = \left(\frac{10LJ}{64\rho^2 v^3} \right)^{1/4} \quad (m = -1/2). \quad (20)$$

The above results obtained from Eqs. 12a and b, under the assumption of an exponential decay for which $C_1 = C_2 = 0$, permit a better understanding of the algebraically decaying jets examined in this paper. Indeed, a careful inspection of Eqs. 12a and b shows that finite non-vanishing values of the integration constants C_1 and C_2 are associated with an algebraic decay of the similar jet velocity

$$f'(\eta) \rightarrow \gamma \eta^{-\alpha} \quad (\eta \rightarrow \infty) \quad (21)$$

with suitably chosen values of $\alpha > 0$. Thus, one immediately obtains

$$C_1 = 2\gamma^2 \quad (\alpha = 1/2, \quad m = -1/3) \quad (22)$$

and

$$C_2 = 9\gamma^3 \quad (\alpha = 2/3, \quad m = -1/2). \quad (23)$$

On the other hand, using the wall boundary conditions (8b, c) and Eqs. 11a and b, the scale constant γ of the algebraic decay (Eq. 21) can be related to the skin friction S of the corresponding flows as $C_1 = S = 2\gamma^2$, and $C_2 = Sf(0) = 9\gamma^3$. In the first case, we obtain from (11a) the basic equation of the Airy jet over an impermeable wall ($f_w \equiv f(0) = 0$) [1] or over a permeable wall ($f_w \neq 0$) [2], respectively

$$f' = S\eta + \frac{1}{2}(f_w^2 - f^2) \quad (24a)$$

where

$$S = 2\gamma^2 \quad (m = -1/3, \quad \alpha = 1/2). \quad (24b)$$

In the second case, Eq. 11b yields the basic equation of the second algebraically decaying jet over a permeable wall, with specified nonzero value of f_w , as reported recently in [3]

$$2ff'' + 2f^2f' - f'^2 = 2Sf_w \quad (25a)$$

where

$$S = \frac{9\gamma^3}{f_w} \quad (m = -1/2, \quad \alpha = 2/3). \quad (25b)$$

We see, therefore, that the skin friction S and the asymptotic scale factor γ of the algebraically decaying

jets are connected to each other by the simple relationships (Eq. 24b) and (Eq. 25b), reminiscent of Eq. 18 for the TAG jet. However, in contrast to the TAG jet, the integrals (15) and (19) become infinite, and thus no further relationship between S and γ can be obtained. Consequently, the algebraically decaying wall jets described by Eqs. 24a, b, 25a and b each represent a one-parameter family of wall-bounded flows. The selection of these jets with well defined skin friction S requires a specification of its asymptotic scale constant γ .

A more straightforward way to accomplish this selection is to specify the asymptotic behavior of the algebraically decaying jets on the scale of the transversal coordinate y by the requirement [1]

$$u \rightarrow \beta y^{-\alpha} \quad (y \rightarrow \infty). \quad (26)$$

Comparing Eqs. 21 and 26, and having in mind Eqs. 6c and 7a, the relationship between α , β and γ

$$\gamma = \frac{1 - \alpha}{2 - \alpha} \frac{\beta}{vL^{\alpha-1}} \quad (27)$$

is obtained. In the sequel, we restrict our consideration of algebraically-decaying wall jets to the Airy jet ($\alpha = 1/2$) streaming over an impermeable wall, as described by Eqs. 24a and b with $f_w = 0$.

Equation 24a is recognized as a Riccati equation which has the explicit solution [1]

$$f(\eta) = (4S)^{1/3} \frac{\sqrt{3}Ai'(z) + Bi'(z)}{\sqrt{3}Ai(z) + Bi(z)}, \quad z = \left(\frac{S}{2}\right)^{1/3} \eta \quad (28)$$

where now a prime denotes differentiation with respect to the argument of the Airy functions, $Ai(z)$ and $Bi(z)$, defined in [13]. Using properties of the Airy functions [13] we obtain from (28) the asymptotic behavior of the jet velocity

$$f'(\eta) \sim \sqrt{S/2} \eta^{-1/2} \quad (\eta \rightarrow \infty) \quad (29)$$

in full agreement with Eqs. 21 and 24b. Also of interest is the magnitude and position of the maximum jet speed, denoted here by f'_{\max} and η^* , respectively, i.e. $f'(\eta^*) = f'_{\max}$. In terms of the variables used here, Weidman et al. [1] reported for $S=2$ the values $\eta^* = 1.19167$ and $f'_{\max} = 1.63719$. Magyari et al. [2] then showed that the following relationship holds

$$\eta^* = \frac{f'_{\max}}{S} + \frac{S}{2(f'_{\max})^2}. \quad (30)$$

As an illustration, in Fig. 1 the similar velocity $f'(\eta)$ of the Airy jet is compared with that of the TAG jet for the same value $S = 2/9$. According to Eqs. 18 and 20 this choice of skin friction coefficient corresponds to the values $f_\infty = 1$ and $J = 64\rho^2 v^3/10L$ for the TAG jet. The corresponding solution of Eq. 17 is then precisely

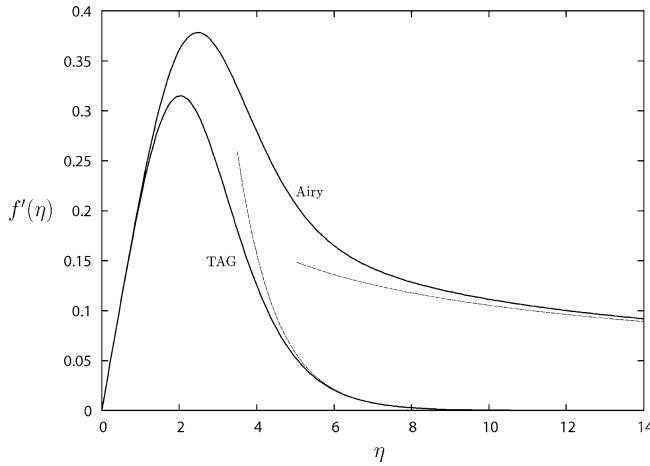


Fig. 1 Similar velocity profiles for the Airy and TAG wall jets for the same value $S=2/9$ of the skin friction parameter. The maximum velocity of the Airy jet exceeds that of the TAG jet by approximately 20%. The *dashed lines* indicate the asymptotic decay of the jet velocities according to Eqs. 29 and 33, respectively

the implicit form given by Glauert [7] (Akatnov [6] used a different normalization), namely

$$\eta = \ln \left(\frac{\sqrt{1+f^{1/2}+f}}{1-f^{1/2}} \right) + \sqrt{3} \tan^{-1} \left(\frac{\sqrt{3}f}{2+f^{1/2}} \right). \quad (31)$$

For the Airy jet, Eq. 24b shows that our choice $S=2/9$ corresponds to $\gamma = 1/3$. This value of γ implies, through Eq. 27, that the reference length L for the Airy jet is related to the asymptotic scale factor β through the expression

$$L = \left(\frac{v}{\beta} \right)^2. \quad (32)$$

The dashed lines in Fig. 1 show the algebraic decay of the Airy jet according to Eq. 29 and the exponential decay of the TAG jet according to

$$f'(\eta) \sim 2\sqrt{3} \exp \left(\frac{\pi}{2\sqrt{3}} - \eta \right) \quad (\eta \rightarrow \infty) \quad (33)$$

obtained from Eq. 31.

5 Temperature solutions

The integral invariant given in (3), evaluated for arbitrary values of m , selects for n the only permitted value

$$n = -\frac{(m+1)}{2}. \quad (34)$$

Thus, $n = -1/3$ for the Airy wall jet ($m = -1/3$) and $n = -1/4$ for the TAG wall jet ($m = -1/2$). Equation 9a for the temperature similarity variable $g(\eta)$ is thereby greatly simplified, resulting in the equation

$$(g' + \text{Pr} f g)' = 0 \quad (35)$$

valid for both wall jets. Two integrations satisfying boundary conditions (Eq. 9b, c) yield the solution in terms of a single quadrature

$$g(\eta) = g(0) \exp \left[-\text{Pr} \int_0^\eta f(\eta) d\eta \right] \equiv g(0) G(\eta) \quad (36)$$

to be evaluated with $f(\eta)$ given explicitly by Eq. 28 for the Airy jet, or implicitly by Eq. 31 for the TAG jet. After a short calculation one obtains

$$G(\eta) = \left[\frac{\sqrt{3} Ai(0) + Bi(0)}{\sqrt{3} Ai(z) + Bi(z)} \right]^{2\text{Pr}}, \quad z = \left(\frac{S}{2} \right)^{1/3} \eta \quad (37)$$

for the Airy jet [4] and

$$G(\eta) = (1 - f^{3/2})^{\text{Pr}} \quad (38)$$

for the TAG jet [8].

In Fig. 2 the similar temperature profiles (Eq. 37) and (Eq. 38) of the two wall jets are compared for different values of the Prandtl number. While for small values of Pr in Fig. 2a the Airy jet temperature profile deviates substantially from that of the TAG jet, with increasing Prandtl number the deviation diminishes such that at $\text{Pr} = 10$ in Fig. 2c the difference is almost imperceptible. It is worth emphasizing here that as $\eta \rightarrow \infty$ the similar temperature field $G(\eta)$ decays exponentially for both jets. Indeed, using the asymptotic behaviors (Eq. 29) and (Eq. 33), one obtains from Eqs. 37 and 38 for $S=2/9$

$$G(\eta) \rightarrow \left[\frac{2\sqrt{\pi}}{3^{1/3}\Gamma(2/3)} \eta^{1/3} \exp \left(-\frac{2}{9} \eta^{3/2} \right) \right]^{2\text{Pr}} \quad (\eta \rightarrow \infty) \quad (39)$$

and

$$G(\eta) \rightarrow \left[3^{3/2} \exp \left(\frac{\pi}{2\sqrt{3}} - \eta \right) \right]^{\text{Pr}} \quad (\eta \rightarrow \infty) \quad (40)$$

for the Airy and TAG jets, respectively. These expressions give a surprisingly accurate approximation to the corresponding exact solutions (37) and (38) even for moderate values of η as shown in Fig. 3 for $\text{Pr} = 0.1$.

In terms of $G(\eta)$, the temperature fields (Eq. 6b) are given by

$$T = T_\infty + T^* g(0) \left(\frac{x}{L} \right)^{-(m+1)/2} G(\eta). \quad (41)$$

The product $T^* g(0)$ of the two unknown constants can uniquely be determined by specifying the incoming heat flux Q_0 and substituting Eqs. 41 and 7a into Eq. 3. The result reads

$$T^* g(0) = \frac{(m+1)Q_0}{2\nu\rho c_p} \theta_w(\text{Pr}) \quad (42)$$

where

$$\theta_w(\text{Pr}) = \left(\int_0^\infty f' G d\eta \right)^{-1}. \quad (43)$$

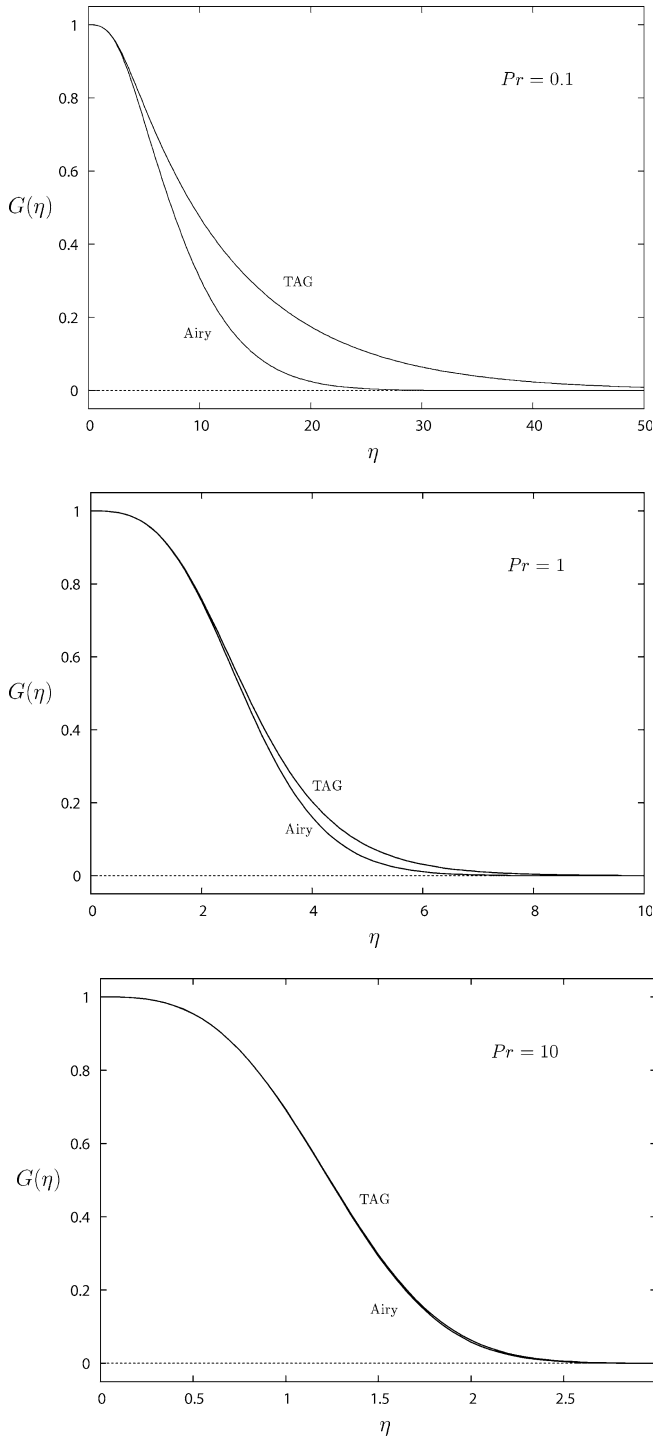


Fig. 2 The similar temperature profiles $G(\eta)$ for the Airy and TAG wall jets for $S=2/9$; **a** $Pr=0.1$, **b** $Pr=1.0$, **c** $Pr=10$

Accordingly, the temperature distribution along the insulated wall below the preheated jet is

$$T_w(x) = T_\infty + \frac{(m+1)Q_0}{2\nu\rho c_p} \left(\frac{x}{L}\right)^{-(m+1)/2} \theta_w(Pr). \quad (44)$$

The thermal quantity of primary interest is the dimensionless function $\theta_w(Pr)$ given by Eq. 43. A comparison

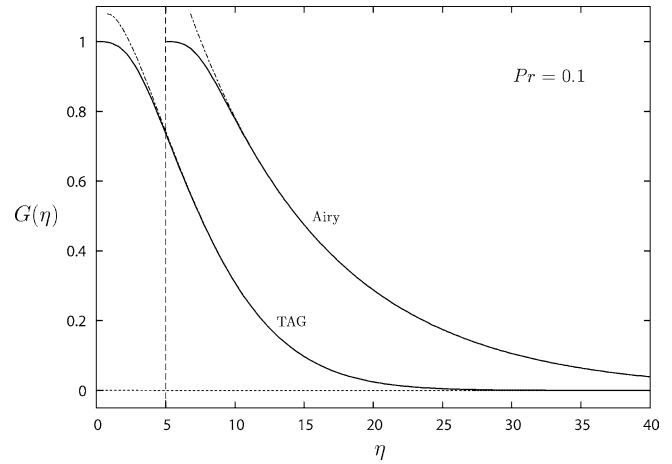


Fig. 3 Comparison for $Pr=0.1$ of the exact similar temperature profile $G(\eta)$ of the TAG jet for $S=2/9$ (solid line) with its asymptotic form (dashed line) given by Eq. 40. For $\eta \geq 5$ the two curves are nearly coincident. The same is shown for the Airy jet for $S=2/9$, but with the origin of η is shifted by 5 units. The asymptotic behavior in the latter case is given by Eq. 39

of this function for the Airy and TAG jets reveals substantial differences at low Pr , and yet striking similarities at large Pr . Equations 37 and 38 show that $G(\eta) \rightarrow 1$ as $Pr \rightarrow 0$ for both the Airy and TAG jets. Thus, from Eq. 43 it follows that

$$\theta_w(Pr) = \lim_{\eta \rightarrow \infty} \frac{1}{f(\eta)} \quad (Pr \rightarrow 0). \quad (45)$$

Hence, to order zero in Pr we obtain

$$\theta_w(Pr) \rightarrow \begin{cases} 0 & \text{(Airy jet)} \\ 1 & \text{(TAG jet)} \end{cases} \quad (Pr \rightarrow 0). \quad (46)$$

On the other hand, for $Pr \rightarrow \infty$, the identical asymptotic behavior

$$\theta_w(Pr) \rightarrow \frac{3Pr^{2/3}}{2\Gamma(2/3)} = 1.10773 Pr^{2/3} \quad (Pr \rightarrow \infty) \quad (47)$$

for the Airy and TAG jets is found. For the TAG jet, the results in Eqs. 46 and 47 are found analytically since in this case Eq. 43 may be evaluated exactly to obtain

$$\theta_w(Pr) = \frac{(2+3Pr)\Gamma(2/3+Pr)}{2Pr\Gamma(2/3)\Gamma(Pr)} \quad (\text{TAG jet}). \quad (48)$$

The TAG jet result (Eq. 46) can be recovered from Eq. 48 since $Pr\Gamma(Pr) \rightarrow 1$ as $Pr \rightarrow 0$, while the TAG jet behavior in Eq. 47 is obtained using Stirling's formula [13]. Moreover, Eq. 48 yields, to first order in the Prandtl number, $\theta_w(Pr) \rightarrow 1 + [3/2 + \gamma + \psi(2/3)]Pr$ where γ is Euler's constant and ψ is the Digamma function, both defined in [13]. Evaluation of the terms leads to the formula $\theta_w(Pr) \rightarrow 1 + 0.758981Pr$ as $Pr \rightarrow 0$.

For the Airy jet, the scaling law (Eq. 47) was confirmed numerically, since apparently no analytical

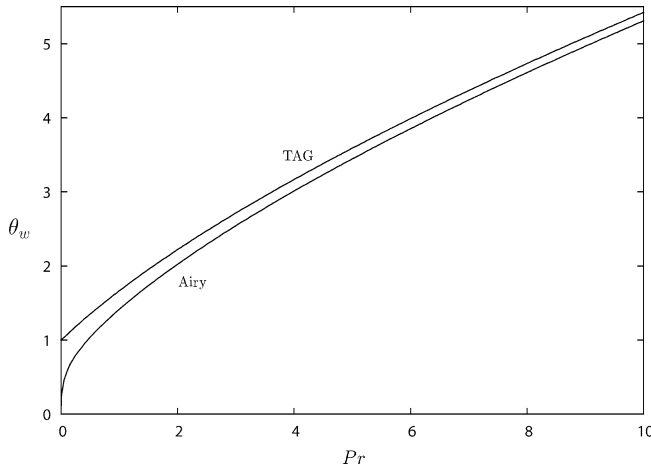


Fig. 4 Dimensionless adiabatic temperature θ_w plotted as a function of the Prandtl number Pr for the Airy and TAG wall jets at $S=2/9$. For large values of the Prandtl number θ_w scales with $Pr^{2/3}$ for both jets, while for small values of the Prandtl number θ_w scales with $Pr^{1/3}$ for the Airy jet and tends to 1 for the TAG jet

expression for the integral (43) is available. For the same reason, the leading behavior $\theta_w(Pr) \rightarrow 1.281954 Pr^{1/3}$ as $Pr \rightarrow 0$ for the Airy jet was obtained numerically. Hence, the leading order Prandtl number behaviors of Eq. 46 are

$$\theta_w(Pr) \rightarrow \begin{cases} 1.281954 Pr^{1/3} & (\text{Airy jet}) \\ 1 + 0.758981 Pr & (\text{TAG jet}) \end{cases} \quad (Pr \rightarrow 0). \quad (49)$$

A comparison of the exact solutions $\theta_w(Pr)$ for the Airy and TAG jets is given in Fig. 4.

6 Conclusion

The flow and thermal characteristics of the algebraically decaying preheated Airy wall jet were investigated and compared in detail to those of the classical exponentially decaying preheated Tetervin-Akatnov-Glauert (TAG) wall jet. These two wall-bounded flows are associated with two respective differential invariants of the corresponding steady velocity boundary-layer equations under affine transformations which, as is well known, represent a continuous symmetry (Lie) group of these

equations. The Airy jet belongs to the similarity class of the Schlichting-Bickley submerged free jet [1] but, in contrast to this and to the exponentially-decaying TAG jet, its far field is an algebraically-decaying rotational flow. Due to this latter circumstance, for the same value of the wall shear stress, the thermally non-preheated Airy and TAG wall jets cannot be distinguished from each other physically by the values of some conserved integral quantities (which for the Airy jet become divergent), but only by the values of their far field behavior. If, however, the Airy and TAG wall jets flowing over an insulated wall are thermally activated by a preheating, their similar temperature fields become quite different for small and moderate Prandtl numbers, yielding in this way a criterion for their distinction.

Acknowledgements P.D.W. extends his gratitude to Professor Bruno Keller for his generous hospitality and support as Visiting Professor in the Department of Building Physics at ETH Zürich during the period this research was conducted.

References

1. Weidman PD, Kubitschek DG, Brown SN (1997) Boundary layer similarity flow driven by power-law shear. *Acta Mech* 120:199–215
2. Magyari E, Keller B, Pop I (2003) Boundary-layer similarity flows driven by a power-law shear over a permeable plane surface. *Acta Mech* 163:139–146
3. Magyari E, Keller B (2004) The algebraically decaying wall jet. *Eur J Mech B/Fluids* 23:601–605
4. Magyari E, Keller B, Pop I (2004) Heat transfer characteristics of a boundary-layer flow driven by a power-law shear over a semi-infinite flat plate. *Int J Heat Mass Transfer* 47:31–34
5. Tetervin N (1948) Laminar flow of a slightly viscous incompressible fluid that issues from a slit and passes over a flat plate. NACA TN 1644, Washington, p 40
6. Akatnov NI (1953) Development of 2D laminar jet along a solid surface. *Leningrad Politekhn Inst Trudy* 5:24–31
7. Glauert MB (1956) The wall jet. *J Fluid Mech* 1:625–643
8. Riley N (1958) Effects of compressibility on a laminar wall jet. *J Fluid Mech* 4:615–628
9. Schwarz WH, Caswell B (1961) Some heat transfer characteristics of the two-dimensional laminar incompressible wall jet. *Chem Eng Sci* 16:338–351
10. Schlichting H, Gersten K (2000) *Boundary layer theory*. Springer, Berlin Heidelberg New York
11. Schlichting H (1933) Laminare Strahlausbreitung. *J Appl Math Mech (ZAMM)* 13:260–263
12. Bickley WG (1937) The plane jet. *Phil Mag* 23:727–730
13. Abramowitz M, Stegun I (1972) *Handbook of mathematical functions*. U. S. Government Printing Office, Washington